Fibers and Polymers 2021, Vol.22, No.10, 2869-2877
DOI 10.1007/s12221-021-0127-6

ISSN 1229-9197 (print version)
ISSN 1875-0052 (electronic version)

The Improved Mechanical and Thermal Properties of Hemp Fibers Reinforced Polypropylene Composites with Dodecyl Bromide Modification

Hongming Wu[1,4]*, Dinghong Xu[1,3], Ying Zhou[1], Jianbing Guo[1,2]*, Weidi He[1], Yong He[2], Yuan Yi[5], and Shuhao Qin[1,2]

[1]*National Engineering Research Center for Compounding and Modification of Polymer Materials, Guiyang 550014, China*
[2]*Department of Polymer Materials and Engineering, College of Materials and Metallurgy, Guizhou University, Guiyang 550025, China*
[3]*State Key Laboratory of Polymer Materials Engineering, Polymer Research Institute of Sichuan University, Chengdu 610044, China*
[4]*Guizhou Material Industrial Technology Institute, Material Technology Innovation Base of Guizhou Province, Guiyang 550014, China*
[5]*School of Materials and Metallurgical Engineering, Guizhou Institute of Technology, Guiyang 550003, China*
(Received September 22, 2020; Revised January 11, 2021; Accepted January 21, 2021)

Abstract: Hemp fibers-reinforced polypropylene (HP/PP) composite is strengthened and toughened by chemical treatment in a melt-blending process. The surface characters of the hemp fibers (HFs) treated by alkaline, γ-valerolactone (GVL) and dodecyl bromide (C12) are studied by FTIR. To evaluate the effect of each chemical treatment on HP/PP composites, the thermal stability, crystalline property, microstructure, mechanical property and rheology property have been studied. It is found that the composites with chemical treatment have improved mechanical property and thermal stability. Among those composites, the tensile modulus and maximum decomposition temperature (T_{max}) of the dodecyl bromide treated composites are highest, and increase 18 % and 10 °C when compared with raw HFs. It is reveals that dodecyl bromide treatment could improve the mechanical and thermal properties of the composites. A possible reinforcing mechanical that hemp fibers react with dodecyl bromide in the composites have been proposed.

Keywords: Natural fiber-reinforced composites, Hemp fiber, Chemical treatment, Interface, Mechanical property

Introduction

Nowadays, with the increased concerns of environment problem and the shortage of non-renewable resource, a lot of attentions are dedicated to use the renewable natural fibers as reinforcement in the thermoplastic polymers [1-5]. The natural fibers reinforced composites (NFCs) have received increasing interests from industry in a wide field of application such as the panel and engine cover in automobile, the door and window frames in the construction, the interior paneling in the aircraft and the decking packing [6,7]. The NFCs have many advantages not only the renewable, inexpensive and low density characters but also no damage to the equipments during the processing while the glass and carbon always do [9,10]. Therefore the NFCs have a bright prospect to replace the synthetic fiber reinforced composites and will be widely used in the future.

However, NFCs also have a certain shortfalls in properties. The main problem of the NFCs is the highly polar surface of NFs that induces an inferior compatibility with non-polar polymer matrix [11-14]. The hydrophilic cellulose structure in the NFs unit is the origin of this problem, because the chemical characters of the NFs and polymer matrix are different and the coupling of those two conflict phases together is also a challenge [15-18]. This defect causes ineffective stress transfer throughout the interface of the composites so a certain modification on the NFs surface is definitely needed. In recent years, different surface modifications have been reported including alkaline treatment [16,19], silicone coupling grafting [12,20], functional plant oil modification [15] potassium permanganate modification [21] and chemical grafting [5,22,23]. Among those treatments, chemical grafting is most effective for the functional modification of the composites. The chemical treatment is usually based on the functional group of reagent that is capable to react with the fiber structure and changing the composition. As a result, the surface chemical characters are changed to facilitate greater compatibility with the polymer matrix.

To get the good adhesion with a hydrophobic polymer, all waxy material and pectin covering on the fiber's surface should be removed beforehand. One goal of the chemical treatment is to remove these non-cellulose components and add functional groups to increase bonding in polymer composites [24]. Some papers have reported the modification of NFs by chemical grafting with the chemical regents in recent years [25-27]. For example, the maleic anhydride grafted styrene-(ethylene-butene)-styrene three-block copolymer (SEBS-g-MA) [28] as a compatibillizer have been used to modify the Moroccan hemp fiber reinforced polypropylene composites to increase the interaction at the interface. The

*Corresponding author: whmand1988@sina.com
*Corresponding author: guojianbing_1015@126.com

functional modified plamitic acid [29] is used to chemically modified Alfa fibers by the esterification between fibers and the functional plamitic acid to improve the mechanical and thermal properties of the composites. However, the study for more effective chemical modification technology to improve the mechanical property and the reinforcing mechanism of the composite interface are also necessary.

This work focuses on the effects of chemical modification on the NFs and the composites properties. Three chemical treatments including alkaline treatment, γ-valerolactone treatment and dodecyl bromide grafting have been used for short hemp fibers (HFs) modification to enhance mechanical properties of the composites. The chemical treated and raw NFs were incorporated into polypropylene (PP) matrix before the tensile specimen was fabricated in a melt-bending process. The modified and unmodified HFs is incorporated at fixed fiber content about 10 %. Though this, the effects of chemical treatment can clearly be evaluated as soon as the melt-blending process can be finely done. In this paper, different chemical regents have been used to treat the HFs to modify the surface property. The hemp fibers treated with chemical regent are incorporated into PP matrix by a melt-blending process. To evaluate the effects of modification on the composites properties, the mechanical property, fractured property, thermal property, crystalline property and rheology properties of the composites have been studied.

Experimental

Material

PP (Sinopec, T30S, a density of 0.9 g/cm^3, melting temperature of 170 °C) was supplied by China Petroleum & Chemical Corporation (Maoming, Guangdong, China). Raw hemp fibers (HFs, 1 mm diameter) were purchased from Yisheng Plant Fiber Co., Ltd. (Shandong, China) and snipped to short fibers with about 10 mm length before use. The chemical used for treatment were NaOH (Sodiun hydroxide, AR, Aladdin, America), GVL (γ-Valerolactone, AR, Aladdin, America) and C12 (dodecyl bromide, 98 %, Aladdin, America). The solvents for remove unreacted chemicals were isopropanol (≥99.9 %, Aladdin, America) and acetic acid (AR, Aladdin, America).

Chemical Treatment of Hemp Fibers

Preparation of NaOH-HP

The raw HFs were first washed with deionized water and then kept for 24 h in a 1.6 mol/l NaOH aqueous solution [30]. The as-treated HFs were removed from NaOH solution and treated with acetic acid to neutralize the residual hydroxide. Finally, those fibers were air-dried at 80 °C for 24 h before use.

Preparation of GVL-HP

Raw HFs were washed with deionized water and soaked in GVL solution at 140 °C for 1 h. The as-treated fibers were removed from the GVL solution and washed with acetic acid to remove the residuals. Finally, the as-treated hemp fibers were dried at 80 °C for 24 h before use.

Preparation of C12-HP

The C12 (3 m*l*) was added into a solution of HFs (5 g) and NaOH (2 g) in 50 m*l* isopropanol. Then the solution was stirred at room temperature for 12 h. The as-treated HFs were removed from the solution and washed with acetic acid to remove the residuals. Finally, the as-treated HFs was dried at 80 °C for 24 h before use.

Preparation of the HP/PP Composites

The as-treated hemp fibers were melt-blended with PP by using a heated two rollmill mixer (Thermo Scientific, America) to prepare the HP/PP composites. The mixing conditions were set at 190 °C for 10 min in each case. These conditions have been selected in order to homogenize the dispersion and the distribution of fibers in the PP matrix. For each case, neat PP was filled onto the rolls and heated to processing temperature. After that, the fibers were slowly added into the melted PP and milled at a constant rotation of 50 rpm for 10 min. In the blended process the torque measured was constant. The blend was removed after the rolls were stopped and the blend was cut into small pieces before injection molding.

The dumbbell and rectangular specimens for characterization were done by a SZS-20 Micro-injection molding machine (Ruiming laboratory apparatus Co., Ltd., WuHan, China). The condition for molding was as following: injection temperature of 200 °C, injection speed of 10 mm/s, injection time of 12 s, mold temperature 40 °C, and cooling time of 30 s. The pieces were added into charging barrel of the machine and heated to 210 °C maintained 5 min before injection molding. The HFs content of the composite was fixed at 10 wt% for easy to process. The neat PP and raw HP/PP blends were prepared as references with the same process. A brief illustration for the preparation of the HP/PP blends is shown in the Figure 1. The compositions of the HP/

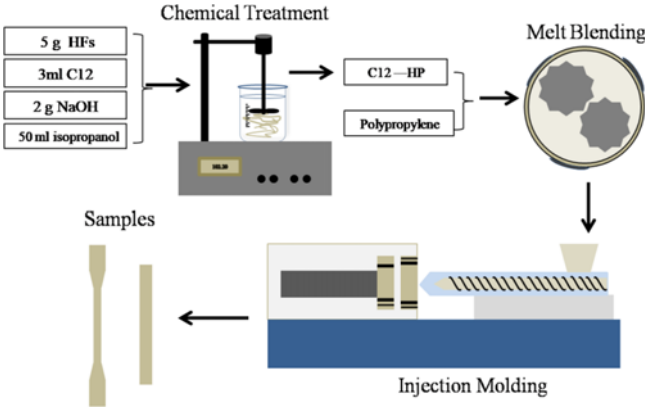

Figure 1. Illustration of prepare HP/PP composites.

Table 1. Composition of the HP/PP composites

Sample	PP (%)	HFs (%)	Notes
Neat PP	100	0	-
Raw-HP/PP	90	10	Untreated
NaOH-HP/PP	90	10	NaOH treated
GVL-HP/PP	90	10	γ-valerolactone (GVL) treated
C12-HP/PP	90	10	dodecyl bromide treated

PP composites are shown in Table 1.

FTIR Analysis

Before FT-IR measurement, the treated HFs was ground and dried at 60 °C for 24 h in vacuum oven. The FT-IR (NEXUS-570 spectrophotometer, Thermo Nicolet Nexus, America) was used to characterize the HFs over a range of 4000-500 cm^{-1} with the resolution and scanning number of 4 cm^{-1} and 32 times, respectively. The samples for FT-IR analysis were prepared by pressing with KBr at a mass proportion of about 1/100.

Scanning Electron Microscopy (SEM)

The microscopic morphologies of the samples were observed with an SEM instrument (Quanta FEG250, FEI) at an acceleration voltage of 25 kV. All samples were cryo-fractured. Before test, the sample surfaces were sputtered with a gold film.

Thermal Gravimetric Analysis (TGA)

TG and TGA tests were carried out by using a Q50 thermogravimetric analyzer (TA Instruments, Thermo, America) that range from room temperature to 500 °C with a heating rate 10 °C/min. In the test process, a continuous high-purged nitrogen atmosphere protect was used.

Differential Scanning Calorimetry (DSC)

The crystallization behaviors of the composites were studied by using a Q10 DSC tester (TA Instruments, Thermo, America). The specimens from injection molding were directly cut into small pieces for test. About 10 mg samples were sealed into an aluminum pan with a lid and an empty hermetic pan was used as a reference. All the measurements were carried out in a N_2 atmosphere. The sample heated from 25 °C to 220 °C at a constant rate of 10 °C/min. According to the DSC results, the crystallinity of PP was calculated according to the following equation [31].

$$X_c = \frac{\Delta H_m}{\Delta H_{100} \times \chi_{PP}} \times 100 \quad (1)$$

where ΔH_m is melting enthalpy, ΔH_{cc} is cold crystallization enthalpy, ΔH_{100} is the theoretical enthalpy of the crystalline PP to melt (206 J/g), and χ_{PP} is the weight ratio of PP in the composites.

Mechanical Testing

A WDW-10C Instron (Hualong Test Instrument, Shanghai, China) was used for tensile and blending measurement following the standard ISO 527-4. The size of dumbbell sample is 75 mm total length, 5 mm narrow section width and 2 mm thickness were used to tensile test with a crosshead speed of 10 mm/min. The size of rectangular sample is 80 mm total length, 10 mm width, and 4 mm thickness. The impact test was performed following the ISO179-1:98. The rectangular samples with a 2 mm notch depth and used an impact tester (Toyoseiki IT, Japan) with A 5.5 J pendulum. All the mechanical tests were conducted at 25 °C with humility of 55 %, and five measurements were conducted for each sample for averaging.

Rheological Property

Dynamic rheological measurements were carried out on a strain controlled ARES rheometer (HAAKE MARS, America) using a 25-mm parallel-plate geometry and a 1-mm sample gap, at frequencies from 0.01 to 100 rad/s in the linear viscoelastic range (strain52%). All measurements were performed under N_2 atmosphere to prevent polymer degradation or moisture absorption.

Results and Discussion

FT-IR Analysis of the Composites

In order to study the influence of chemical treatment on the surface structure of HFs, the FTIR spectra of as-treated HFs have been obtained. Figure 2 show the FT-IR spectra of raw HFs and as-treated HFs. The spectra of the HFs treated with different chemical reagents show the similar peaks at the range from 800 cm^{-1} to 4000 cm^{-1} while some characteristic peaks of the treated HFs are uniquely for distinguish the surface structure of raw HFs. All the samples own the HFs characteristic peaks, as the characteristic peaks at 3424 cm^{-1} and 1586 cm^{-1} are ascribe to the -OH stretching and C=C

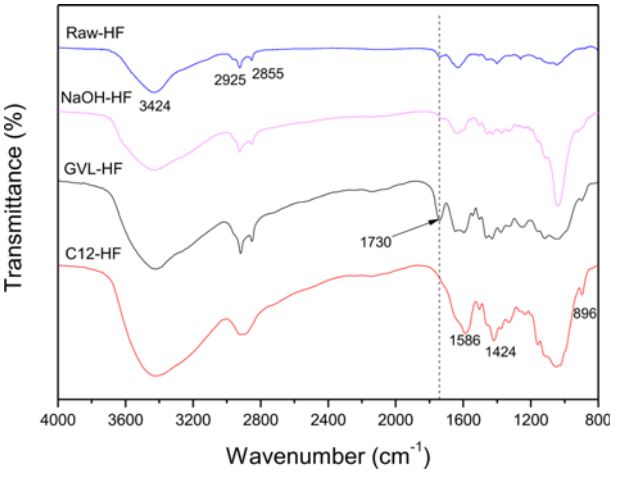

Figure 2. FT-IR spectra of the treated hemp fibers.

stretching of the HFs and peaks at 2925 cm^{-1} and 2855 cm^{-1} are attributed to -CH_2- and -CH_3 stretching vibration in the HFs [9,32]. However, a distinct absorption peak at 1730 cm^{-1} that correspond to (C=O) strengthening is different and it is found to depend on fiber modification. The C=O strengthening in γ-valerolactone treated HFs (GVL-HP) is significantly higher than that of raw HFs because some ester group maybe exist by the GVL absorbing on the surface of the HFs. For the spectrum of alkaline treated HFs (NaOH-HP), the C=O strengthening is less than the raw HFs that may due to the sodium hydroxide solution to dissolve and removal of non-cellulosic impurities such as pectin and hemicelluloses from the surface [33-35].

It is interesting that the spectrum of dodecyl bromide treated HFs (C12-HP) is distinguishable from that of untreated HFs as the carboxyl stretching shoulder at about 1730 cm^{-1} is disappeared because the noncellulose impurity in the native HFs are removed by the solution [32]. While the observed peaks at 1424 cm^{-1} and 896 cm^{-1} that attribute to the CH_2 symmetric bending are increased, as the symmetric in-phase strengthening in the treated HFs, that reveals the dodecyl bromide reacts with hydroxyl group on the surface of the HFs [36]. As a result, the linear chain may graft on the HFs to modify the surface chemical structure of the HFs.

SEM Analysis

The microstructures of the treated-HP/PP composites have been studied by SEM. Figure 3 show the cryo-fractured surface of neat PP and the treated HF/PP composites. In neat PP, the cryo-fracture surface is flat reveals the integrity of PP matrix. When raw HFs incorporated into the PP matrix, some grooves and splits can be observed on the interface. The fiber bundle randomly immerged in the PP matrix with some ravines reveal the inferior interface compatibility. When the treated HFs are incorporated into PP matrix, the interface compatibility improved obviously as shown in Figure 3(c) to 3(e). The fractured surface of the C12-HP/PP composite shows a fantasy interface adhesive. There are no HFs pull out and some broken HFs can be observed on the flat surface of matrix. The GVL and NaOH treated HFs also show the improved interface property. As a result, the interface compatibility of the composite has been improved by chemical treatment and the HFs is the main force-bearing for the composites.

Thermal Stability

Thermal stability of the composite is invested by the thermogravimetric analyzer. The TG and DTA curves are shown Figure 4. The TG curves of all the composites show several loss stages. The first weight loss between 50 °C to 170 °C is generally corresponding to water loss in the composites. In all composites, there exists a main mass-loss region that always located between 400 °C to 470 °C in the curves as presented in Figure 4a). This region may be attributed to the thermal decomposition of PP matrix. Moreover, the C12-HP/PP composite shows a mass-loss stage before PP matrix decomposition that maybe attributed to the deformation of the dodecane bromide molecule.

The DTA peak temperatures of the treated HP/PP composites are shown in the Figure 4(b). The T_{max} of raw HP/PP about 449 °C is lowest in all the composites and the

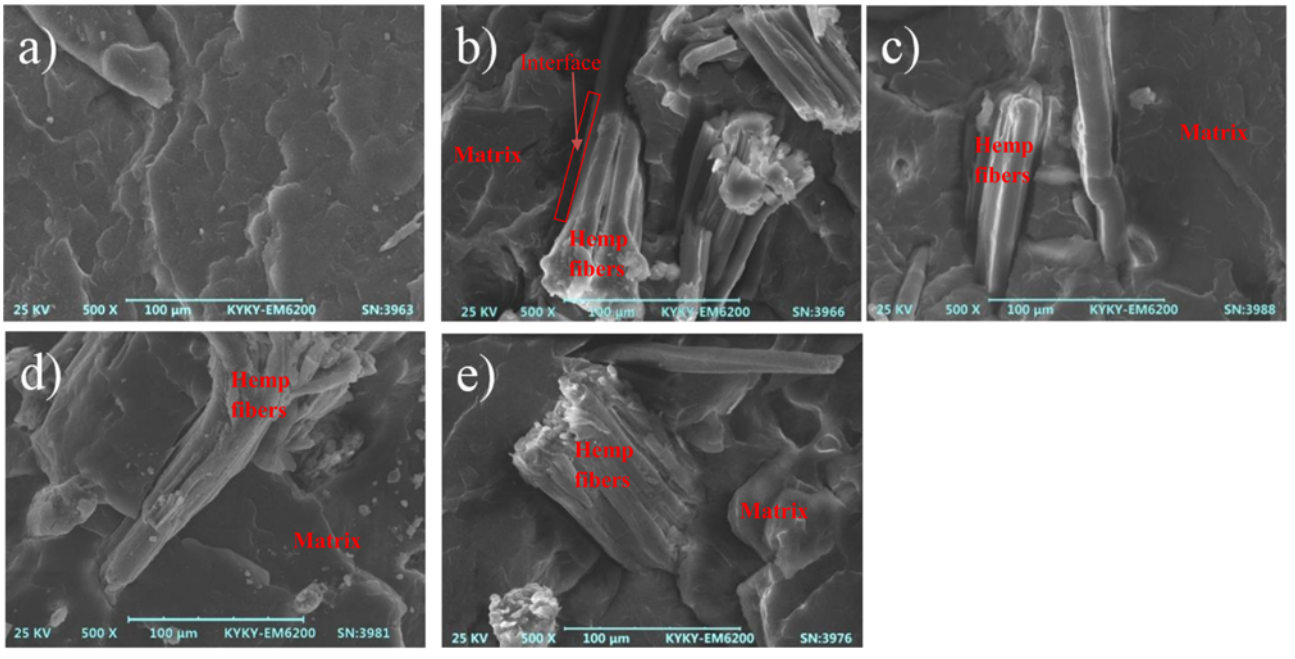

Figure 3. SEM images of the composites; (a) neat PP, (b) raw HP/PP, (c) GVL-HP/PP, (d) NaOH-HP/PP, and (e) C12-HP/PP.

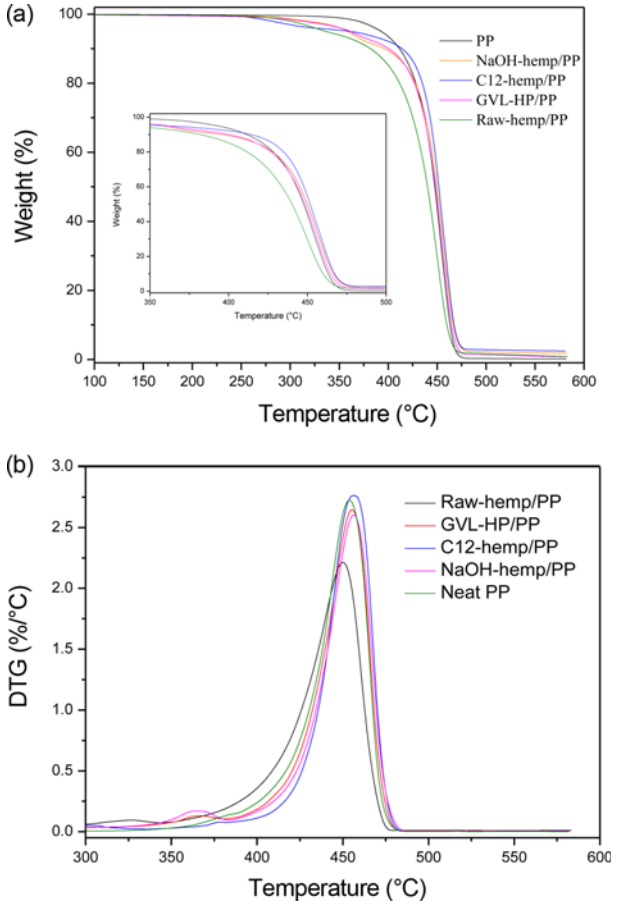

Figure 4. TG (a) and DTA (b) curves of the treated HP/PP composites.

T_{max} of C12 treated HP/PP composite shift to higher temperature that is about 457 °C. It is interesting that compared with non-treated HP/PP composite, the T_{max} of treated HP/PP composites increase about 10 °C that reveals the improved thermal stability. The GVL treated HP/PP composite show a slightly decrease in the decomposition temperature because the ester bond is formed in the composite after treatment which is sensitive to contact to humility or oxygen, while the ether bond formed in C12 treatment is difficult to break in the same condition [27]. In the DTA curves, the GVL-HP/PP and C12-HP/PP composites have a small heat flow platform at the region of 350 °C to 360 °C which may attribute to the decomposition of dodecane bromide and GVL. The T_{onset} of treated HP/PP and raw HP/PP composites are less than the neat PP that may be responsible for the HP/PP composites processing. As the melt-blending process always used friction forcing between hemp fiber and polymer matrix to mixture together resulting in a possible breakage of polymer chain that induce a decrease in the thermal stability. The detail thermal properties of the treated HP/PP composites are shown in Table 2.

Table 2. Thermal properties of the composites

Sample	T_{onset} (°C)	T_{max} (°C)	Residual (%)
Neat PP	393.0	454.14	0.12
Raw-HP/PP	336.5	449.84	0.78
NaOH-HP/PP	361.1	455.22	2.38
GVL-HP/PP	361.3	455.22	0.75
C12-HP/PP	359.1	456.29	1.70

Crystalline Property

The thermal transition behavior of the composites is invested by DSC scans. Figure 5 show the DSC curves of the treated HP/PP composites. All the composites show a similar endothermic curve with peak temperature about 164 °C. The temperature of endothermic peak is comparable with that of neat PP reveal the incorporated HFs has little effects on the crystalline property. For the exothermic curves of the composites as shown in Figure 5(b), the exothermic peak temperature of raw HP/PP composite is about 120 °C which is higher than that of neat PP that is about 115 °C.

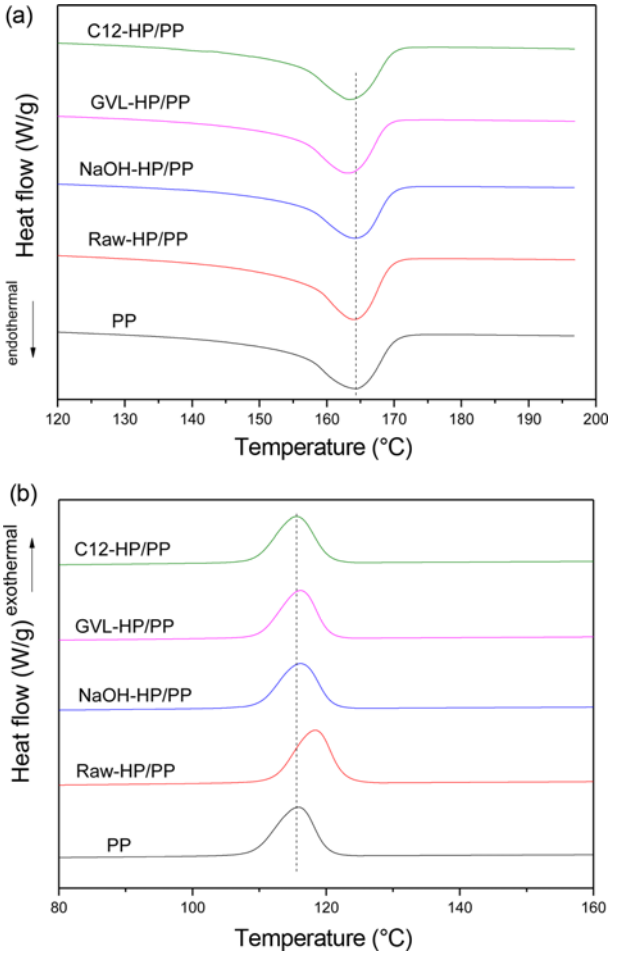

Figure 5. DSC curves of neat PP and the treated HP/PP composites.

Table 3. Crystalline property of the treated hemp fiber composites

Sample	ΔH_{cc} (J/g)	T_{cc} (°C)	ΔH_m (J/g)	T_m (°C)	χ_c (%)
Neat PP	115.4	115.86	101.0	164.32	48.79
Raw-HP/PP	121.5	118.36	109.3	164.03	58.67
NaOH-HP/PP	106.7	116.19	96.44	164.16	51.76
GVL-HP/PP	105.1	116.16	93.67	163.15	50.28
C12-HP/PP	105.9	115.56	94.30	163.42	50.61

Similarly, the exothermic peak temperature of the treated HP/PP composites is also comparable with neat PP, while the raw-HP/PP composite is about 120 °C higher than that of the treated HP/PP composite. This implies that the uniformity microstructure of the treated HP/PP composites is improved. According to the crystalline property of the treated HP/PP composites as shown in Table 3, the T_c and χ_c for GVL and C12 treated HP/PP composites are lower than that of the NaOH treated and raw HP/PP composites. This may be ascribed to the chemical bond on the interface of the composite limited the crystallinity.

Mechanical Property

Figure 6 shows the stress-strain curves of the treated HP/PP composites. All of the stress-strain plots for the composites are similar with a yield point apparently. It can be seen that the yield strength (YS) of the treated HP/PP composites are much higher than that of raw HP/PP composite. This proves the improved fibers-matrix interface adhesion duo to the grafted effects on the HFs. The YS of neat PP is about 32.5 MPa while that of raw HP/PP composite decrease to about 30 MPa. This may be ascribed to the incorporated HFs destroyed the integrity of PP matrix in a melt blending process hence the YS decreased. When the HFs were chemical treated, the YS of the composites increased obviously. In the treated HP/PP composites, the C12-HP/PP composite is highest that is about 37 MPa which

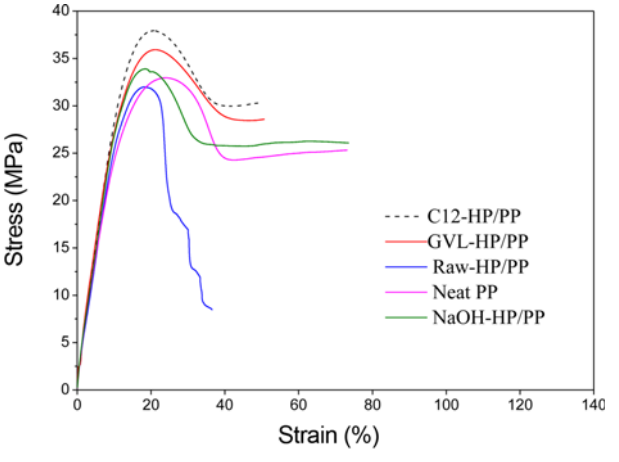

Figure 6. Stress-strain curves of the treated HP/PP composites.

increase about 18 % compare with raw HP/PP composite. The increased YS may be attributed to dodecyl bromide react with the hydroxyl on the HFs to form a stable chemical bond hence improve the compatibility between the HFs and PP matrix.

The tensile, bending and impact properties of treated HP/PP composites are shown in Figure 7. To the tensile property, it can be seen that there is a considerable increase for Yong's modulus reach to 700 MPa in the C12-HP/PP composite much higher than raw HP/PP composite and neat PP that is about 400 MPa. The similar trend to the situation also can be

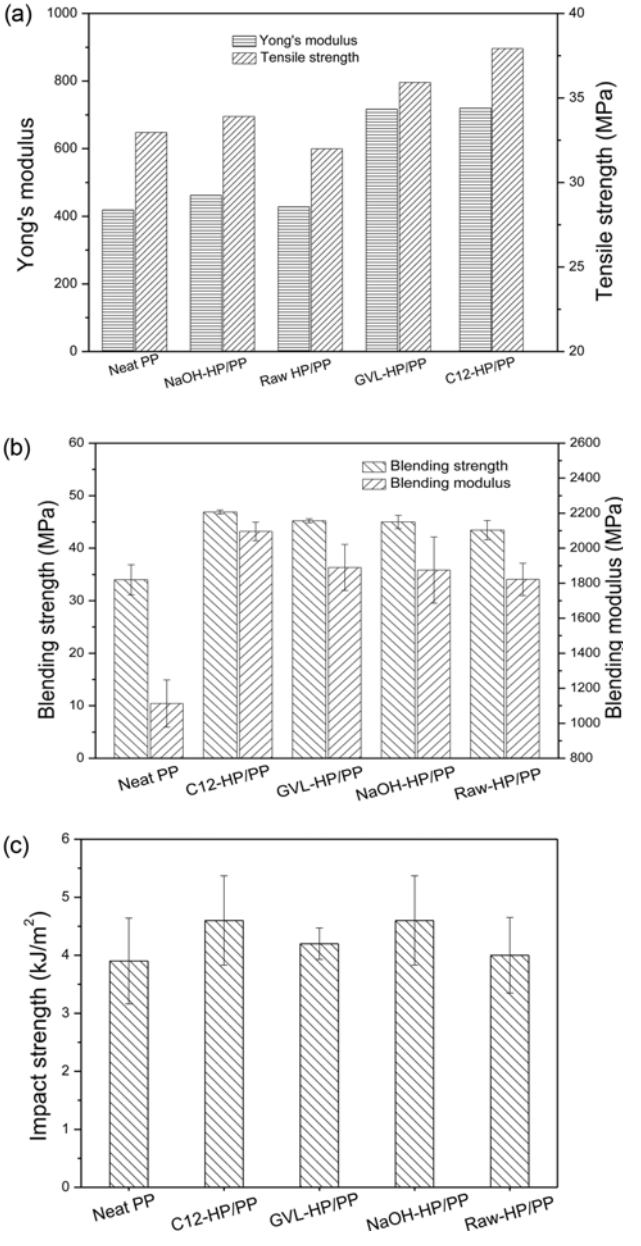

Figure 7. Testing results of the tensile (a), bending (b), and impact (c) properties of the composites with different treatments.

seen in the tensile strength (TS) of the composites. For the bend property as shown in Figure 7(b), the HFs incorporated composites own higher bending strength (BS) and bending modulus (BM) than neat PP that may be attributed to the HFs reinforcement improve the strength and stiffness. Moreover, the BS and BM of treated HP/PP composites are also higher than raw HP/PP composite for the improved interface adhesion. The impact strength (IS) of the composites is comparative with neat PP as shown in Figure 7(c) that reveals the chemical treatment have little effects on the IS of the composites. It is interesting that the TS and BS of the C12-HP/PP are biggest in all the composites because reaction between dodecyl bromide and hydroxyl group on HFs enhance the compatibility of the composites.

Reinforcing Mechanism of the Composites

In order to investigate the reinforcing mechanism of the dodecyl bromide treatment on the composites, the tensile-fractured surface had been invested by SEM scan. Figure 8 shows the internal morphology for the stretched sample and a possible reaction on the HFs have been proposed.

In the C12-HP/PP composites, the raw fibers were treated by NaOH solution to remove the hemicellulose and non-cellulosic impurities pectin of fibers on the surface. The exposed cellulose with the hydroxyl groups could reactive with NaOH molecules and form a intermediate (hemp fiber-O^-Na^+) in the solution [27,37]. When the dodecyl bromide added into the solution, it could react with the intermediate by a replacement reaction and an ester bond has been formed. As a result, the linear chain from dodecyl bromide grafted on the HFs by an esterification reaction that improved the hydrophobicity of the HFs because of the special characteristics of dodecyl bromide [29]. In this reaction the NaOH was act as a catalys. When melt blending, the dodecyl bromide grafted HFs will have a good compatibility with the PP matrix that improve the interface property of the composites. According to the internal morphology of the stretched sample, the vertical direction of the sample present some fractured fibers indicate that the fibers is main force bearing (Figure 8a). From the stretched direction, a large number of highly oriented fibers with high aspect ratio can be observed (Figure 8b). As proposed in Figure 8b, when tension loaded, the randomly distribute fibers in original composites start to deform and array orderly along the stretching direction and act as the major force bearing. Meanwhile the matrix around fibers will orientate form the fibers when stress is higher than the interface adhesion. As a result, generation of fibers fractured and matrix plastic deformation increase shear yielding strength.

Rheological Property

The rheological property of polymer is important for the practical processing and application. Figure 9 shows the storage modulus (G′), loss modulus (G″) and complex viscosity (η^*) of the treated HP/PP composites at different frequencies. It is can be seen that all the composites present similar G′ and G″ variation trends in the invested frequency. Both G′ and G″ increase with the rotational frequency as shown in Figure 9(a) and 9(b) because of the typical pseudoplastic fluid characteristic of the composites [38,39]. Furthermore, the G′ and G″ of the C12 treated HP/PP composite are higher than the raw HP/PP composite while the GVL or NaOH treated HP/PP composites are lower. This may be responsible for the C12 molecule with a long linear chain contact with HFs by chemical bond to limit the movability of the polymer chains [10,40]. However, the GVL or NaOH molecule doesn't have strong limit to the polymer chains but act as impurity to increase the movement. Generally, the NaOH solution can dissolve the impurity of the HFs and make the fiber slender and smooth so the G′ and G″ of the composites slightly decreased.

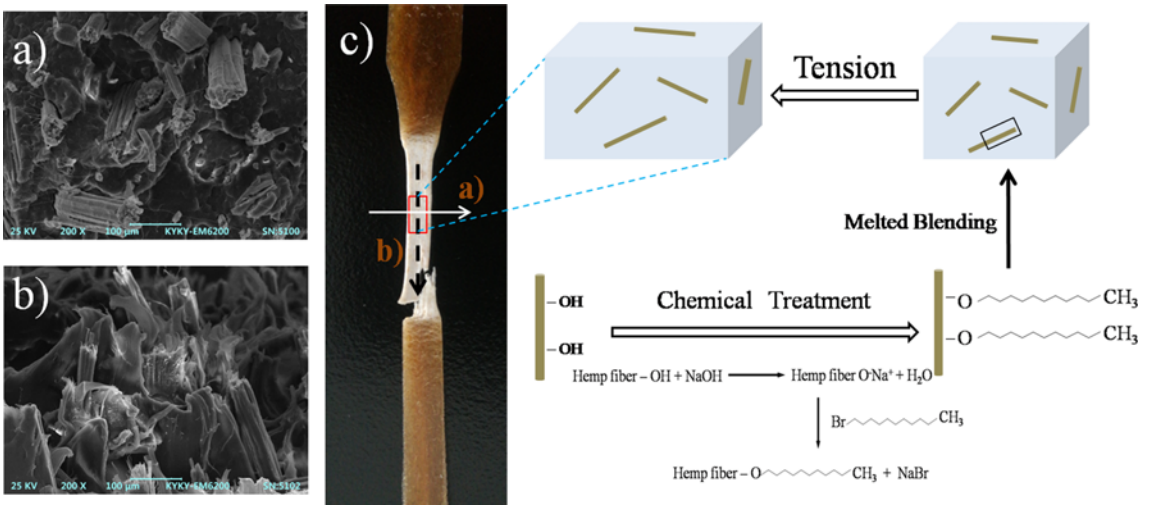

Figure 8. SEM images of stretched samples of C12-HP/PP composites from different perspectives and proposed mechanism during tension.

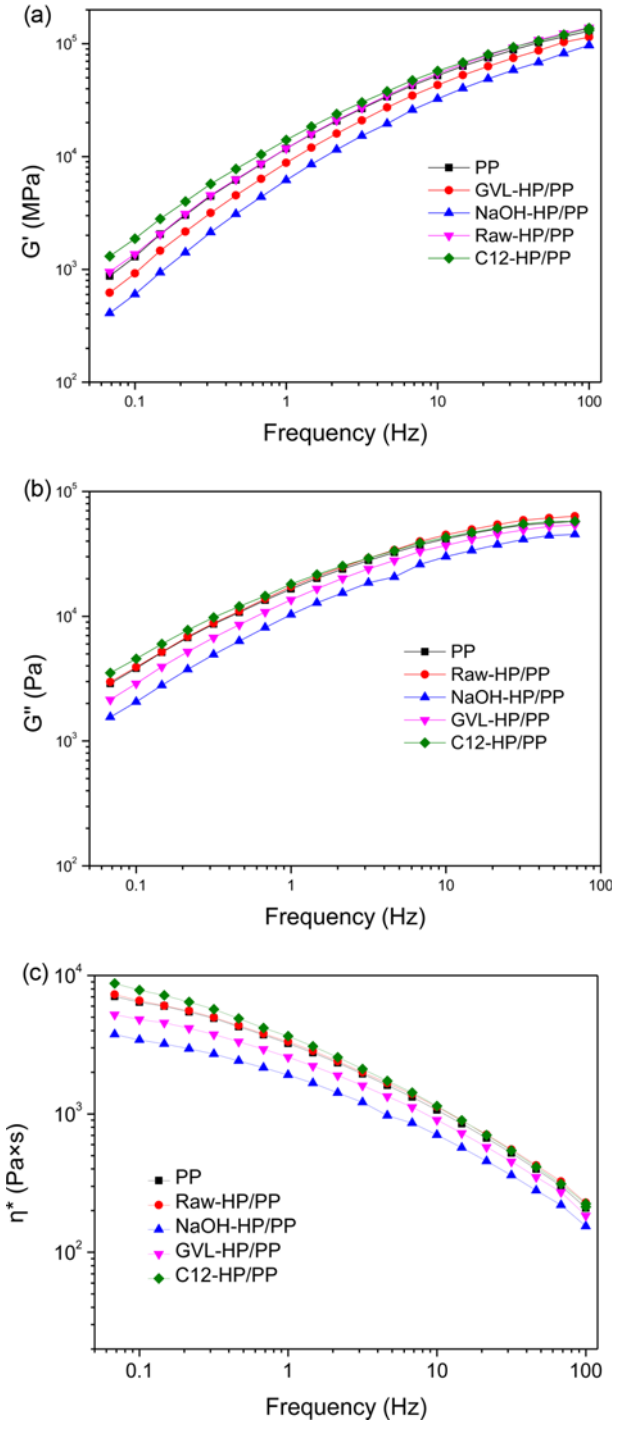

Figure 9. Storage modulus (a), loss modulus (b), and complex viscosity (c) of the HP/PP composites at different frequencies.

Figure 9(c) depicts the shear viscosity as a function of frequency for the treated HP/PP composites. All the samples show the shear shinning behavior in the invested range. When the raw HP incorporated into the PP matrix, the η^* curve of the composite almost overlap with the neat PP that reveals the raw HP has little effects on the PP matrix. Interestingly, the η^* values of the treated C12-HP/PP composites are higher than that of neat PP because the dodecyl bromide could contact with HFs and twine with the PP molecule chain in the melt-blending process [38]. However, the NaOH and GVL treated HP/PP composites show lower viscosity than the raw HP/PP composites because the dissolution in the NaOH solution dismissed the bonding strength of the composites.

Conclusion

In this paper, the HFs are treated with different chemical regents and the HP/PP composites have been prepared via a melt-blending process. The FT-IR spectra of the treated HFs show that the functional groups are grafted on the HFs by chemical reaction. The C12-HP/PP owns the highest tensile strength and bending modulus that increase about 18 % compare with raw HP/PP composite. This is ascribe to the chemical treated HFs have better interface compatibility and act as the main force-bearing in the composites according to the fractured surface and tensile-fractured surface SEM analysis. A noticeable increment (about 10 °C) for T_{max} of treated HP/PP composites can be observed when compare with non-treated HP/PP composite that reveals the improved thermal stability. The rheology property shows that C12 treated HFs composite has a higher storage modulus, loss modulus and complex viscosity than the raw HP/PP composite because of molecule chain interaction in the melt blending process.

Acknowledgement

This work is financially supported by National Natural Science Foundation of China (51602067), Program of Application and Industrialization of Scientificand Technological Achievements of Guizhou (2016-4538), High-level Innovative Talents Training Project of Guizhou (2016/5667), Science and Technology Funds of Baiyun District of Guiyang (2019/22), The Guizhou Provincial Science and Technology Project (Qian Ke He Zhi Cheng[2019]2849), Science and Technology Foundation of Guizhou (2018/1087), Science Corporation Foundation of Guizhou (2019/5635, 2019/2830).

References

1. H. Ku, H. Wang, N. Pattarachaiyakoop, and M. Trada, *Compos. Part B-Eng.*, **42**, 856 (2011).
2. R. Arnaud, T. Maxime, and J. J. Pierre, *Compos. Sci. Technol*., **182**, 107755 (2019).
3. X. Shen, J. Jia, and C. Chen, *J. Mater. Sci.*, **49**, 3225 (2014).
4. M. S. Islam, K. L. Pickering, and N. J. Foreman, *Compos. Part A: Appl. S.*, **41**, 596 (2010).

5. J. F. Pereira, D. P. Ferreira, J. Bessa, J. Matos, F. Cunha, Isabel Araújo, L. F. Silva, E. Pinho, and R. Fangueiro, *Polym. Compos.,* **40**, 3472 (2019).
6. T. Fulga, Z. Madalina, and T. Carmen-Alice, *Polym. Compos.,* **42**, 5 (2020).
7. M. Ramesh, *Prog. Mater. Sci.,* **102**, 109 (2019).
8. Q. Hfm de, B. Md, and C. Dkk, *J. Comp. Mater.,* **54**, 1245 (2019).
9. W. Paul, I. Jan, and V. Gnaas, *Compos. Sci. Technol.*, **63**, 1259 (2003).
10. X. Zhang, X. Wu, H. Haryono, and K. Xia, *Carbohydr. Polym.*, **113**, 46 (2014).
11. X. Li, L. G. Tabil, and S. Panigrahi, *J. Polym. Environ.,* **15**, 25 (2007).
12. A. Atiqah, M. Jawaid, M. R. Ishak, and S. M. Sapuan, *J. Nat. Fibers,* **15**, 251 (2017).
13. S. Bolduc, K. Jung, P. Venkata, and M. Ashokcline, *J. Reinf. Plast. Comp.,* **37**, 1322 (2018).
14. I. Kellersztein and A. Dotan, *Polym. Compos*., **37**, 2133 (2016).
15. Z. Xiong, C. Li, S. Ma, and J. Feng, *Carbohydr. Polym.,* **95**, 77 (2013).
16. L. Fang, L. Chang, W. Guo, Y. Chen, and Z. Wang, *Appl. Surf. Sci*., **288**, 682 (2014).
17. S. O. Amiandamhen, M. Meincken, and L. Tyhoda, *Fiber. Polym*., **21**, 677 (2020).
18. L. Mei, Y. Ren, and G. Guo, *ACS Appl. Mater. Interfaces*, **10**, 42992 (2018).
19. A. M. Radzi, S. M. Sapuan, M. Jawaid, and M. R. Mansor, *Fiber. Polym*., **20**, 847 (2019).
20. K. E. Okon, F. Lin, Y. Chen, and B. Huang, *Carbohydr. Polym*., **164**, 179 (2017).
21. L. He, W. Li, D. Chen, and G. Lu, *Polym. Compos.,* **39**, 3353 (2018).
22. M. L. Troedec, D. Sedan, C. Peyratout, J. P. Bonnet, A. Smith, R. Guinebretiere, V. Gloaguen, and P. Krausz, *Compos. Part A-Eng*., **39**, 514 (2008).
23. C. Lacoste, R. E. Hage, A. Bergeret, S. Corn, and P. Lacroix, *Carbohydr. Polym*., **184**, 1 (2018).
24. W. Liu, J. Qiu, T. Chen, and M. Fei, *Compos. Sci. Technol*., **181**, 107709 (2019).
25. E. A. Al-Mulla, Y. Jaffar, and M. Wan, *J. Mater. Sci*., **45**, 1942 (2010).
26. A. V. Alankar, G. Marc, and A. S. Dawn, *Carbohydr. Polym*., **136**, 1238 (2016).
27. J. Guo, J. Wang, Y. He, and Q. Zheng, *Polymers,* **12**, 632 (2020).
28. A. Elkhaoulani, F. Z. Arrakhiz, K. Benmoussa, R. Bouhfid, and A. Qaiss, *Mater. Des.,* **49**, 203 (2013).
29. F. Z. Arrakhiz, M. Elachaby, R. Bouhfid, and S. Vaudreuil, *Mater. Des*., **35**, 318 (2012).
30. M. Le Troëdec, A. Rachini, C. Peyratout, S. Rossignol, and E. Max, *J. Colloid. Interf. Sci.,* **356**, 303 (2011).
31. W. Liu, J. Qiu, L. Zhu, and M. Fei, *Polymer,* **148**, 109 (2018).
32. W. Liu, T. Xie, and R. Qiu, *Cellulose*, **23**, 2501 (2016).
33. L. Xue, G. T. Lope, and P. Satyanarayan, *J. Polym. Environ.,* **15**, 25 (2007).
34. S. Ouajai and R. A. Shanks, *Polym. Degrad. Stabil*., **89**, 327 (2005).
35. H. G. Higgixs, C. R. I. Stewart, and K. J. Harringtos, *J. Polym. Sci. Polym. Chem*., **51**, 59 (1961).
36. J. Guo, X. Chen, and J. Wang, *Polymers*, **12**, 56 (2020).
37. R. Sepe, F. Bollino, L. Boccarusso, and F. Caputo, *Compos. Part B-Eng*., **133**, 210 (2018).
38. Y. Zhou, Y. He, and H. Wu, *Polym. Compos.,* **41**, 3227 (2020).
39. H. Wu, D. Xu, and Y. Zhou, *Fiber. Polym*., **21**, 2084 (2020).
40. R. Moriana, F. Vilaplana, S. Karlsson, and A. Ribes-Greus, *Compos. Part A-Appl. S.,* **42**, 30 (2011).